LINE MATCHING FROM MULTIPLE AERIAL IMAGES FOR BUILDING RECONSTRUCTION

Jou-Yu Yen*[a] and Liang-Chien Chen[b]

[*a] Graduate Student, Department of Civil Engineering, National Central University,
No.300, Jhongda Rd., Jhongli City, Taoyuan County 32001,Taiwan; Tel: +866-3-4227151ext 57623;
E-mail: geo0313@hotmail.com
[b] Professor, Central for Space and Remote Sensing Research, National Central University,
No.300, Jhongda Rd., Jhongli City, Taoyuan County 32001,Taiwan; Tel: +866-3-4227151ext 57622;
E-mail: lcchen@csrsr.ncu.edu.tw

KEY WORDS: Line matching, Left-right matching, Multi-plane intersection

Abstract: Three dimensional reconstructions is an important task in the field of geospatial information sciences. Image matching is one of essential technology to locate conjugate features including points, lines, and polygons in multi-angle images. Line matching plays an irreplaceable role in man-made scenes, since most of such objects mainly consist of line segments. The purpose of this study is to match lines with the approach of Left-right matching (LR matching) and then reconstruct building models using 3D line segments that are derived from the multi-plane intersection.

There are four steps in the proposed method: (1) line features extraction, (2) straight lines detection, (3) line matching, and (4) multi-plane intersection. First, line features are extracted using Canny edge detector and the straight lines are then detected by Hough transform in each image. After the extraction, we select those lines of interest on master image, and then using epipolar constraint to identify the line candidates on slave images. The next step matches line with LR matching which is to compare the similarity of line neighboring regions. And then we can use multi-plane intersection to reconstruct 3D line segments. The model can thus be reconstructed, accordingly. The preliminary results show that the proposed method is applicable.

1. INTRODUCTION

Three dimensional reconstruction is an important task in the field of geospatial information sciences. For 3D analysis, image matching is one of essential technology to find conjugate features including points, lines, and polygons in multi-angle images. Line matching plays an irreplaceable role in man-made scenes, since most of such objects mainly consist of line segments. Many approaches for line matching have been developed in past decades. The general strategy in most of studies matched the geometry of line segments such as orientation, length, extent of overlap, mid-point, etc. Some studies considered the intensity around the line segments, additionally [Schmid and Zisserman, 1997]. However, the ambiguity problem of line matching is still an issue due to various reasons such as inconsistency of line endpoint locations, partial occlusions, lack of rich textures in line local neighborhood, etc [Ok et al., 2010].

With the development of airborne digital sensor, the overlap of aerial images from same and neighbor strips can reach 80% and 30% or even more. The same object may appear on multiple images which provide more observations for intersection positioning. Thus, we used multiple images with area-based matching in this study. For building reconstruction, we need to extract line features from the edge of the building that are usually located at the elevation discontinuity. The different view angles of sensor may lead to ambiguity matching in elevation discontinuity, since the neighboring regions of line segments may cover different background. Therefore, referring to the strategy of Central-Left-Right matching (CLR matching) [Hsu, 1990], we propose the approach of Left-Right matching (LR matching) to match lines.

The proposed scheme comprises four parts, (1) line features extraction, (2) straight lines detection, (3) line matching, and (4) multi-plane intersection. First, line features are extracted using Canny edge detector [Canny, 1986] and the straight lines are then detected by Hough transform [Hough, 1962] in each image. After the extraction, a similar matching strategy proposed by Ok et al. [2010] is employed in this study. We select those lines which have orthogonal properties to each other on the master image, and then using epipolar constraint to identify the candidate lines on slave images. The next step matches line with LR matching which is to compare the similarity of grey values around line neighboring regions. And then we can use multi-plane intersection to reconstruct 3D line segments.

2. METHODS AND EQUATION

The proposed scheme comprises of four parts: (1) line features extraction, (2) straight lines detection, (3) line matching, and (4) multi-plane intersection. The flow chart of the proposed method is shown in Figure1.

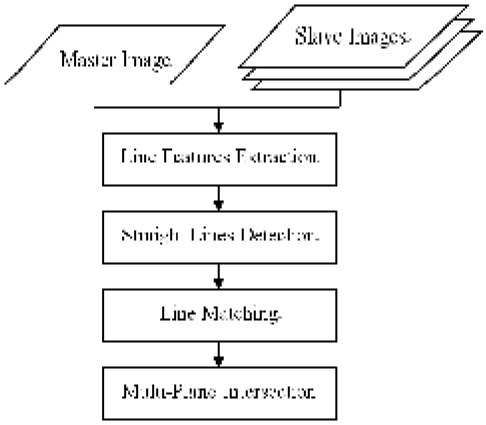

Figure 1: Flow chart of proposed method

Line Features Extraction and Straight Lines Detection

To construct the 3D lines segments of the building edges, we use Canny edge detector to perform the line features on each image. Since the line features may include straight lines and curves, and the most of buildings are consisted of the former type, Hough transform is employed to detect the straight lines after the edge extraction.

Line Matching

Once the straight lines are detected, similar matching strategies proposed by Ok et al. [2010] are employed in this study. The strategy in line matching consists of three stages: (1) selection of the interest lines on master image, (2) identifying the candidate lines on slave images, and (3) Left-right matching.

Selection of the interest lines on master image: Since the straight lines are not only extracted from the building, also from the objects on the ground or others, we have to filter those lines using two criteria: angle between lines and the distance from endpoints to another line. The first criterion, using the properties that the most of building line features is orthogonal to each other. If the angle between two lines satisfies the range of threshold, we keep them. For the second criterion, the endpoints of lines must be close enough to each other. Therefore, the number of line candidates can be reduced. The illustration of two criteria is shown in Figure 2.

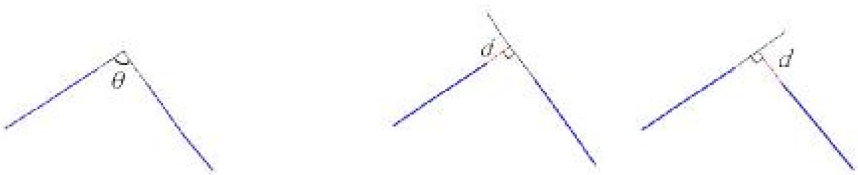

(a) (b)

Figure 2: Two criteria (a) angle between lines, (b) the distance from endpoints to another line.

Identify the candidate lines on slave images: After the interest lines are selected from the master image, the candidate lines on slave images are searched using epipolar constraint. With the initial height information derived from DSM and DEM data, a quadrilateral region constraint generated using the epipolar geometry can be employed to reduce the search space [Suveg and Vosselman, 2004]. Also, only the search lines with the same orientation of master line would be kept as candidates. The illustration of epipolar constraint is shown in Figure 3.

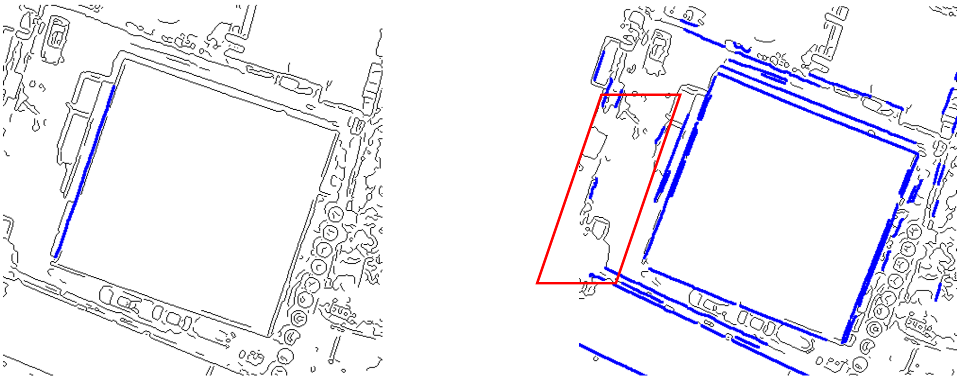

(a) (b)

Figure 3: Epipolar constraint for identifying candidate lines,
(a) interest line on master image (b) quadrilateral region constraint on slave image.

Left-right matching: The different view angles of sensor may lead to ambiguity matching in elevation discontinuity, since the neighboring regions of line segments may cover different background. Therefore, we use the approach of Left-Right matching (LR matching) to match lines. The strategy in LR matching is to compare the neighboring region of the line segments. Since line segments endpoints are different on each image, we can cut or fill using the epipolar constraint to make them consistent with the master image line segments. The consistency of line segments endpoint is shown in Figure 4. Blue line represents the line segments on master image, and red lines are the candidate lines selected on slave image.

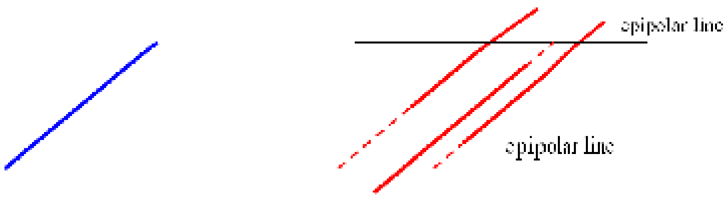

Figure 4: The consistency of line segments endpoint.

We open the left and right window on each side of the line segments in master image. The illustration is shown in Figure 5. The window size is M x N, where M means the number of pixels along the line segments and N represents the half number of pixels across the line segments. After the window determination on the master image line segments, we open two windows on each side of their line candidates. Because the M values are determined by the length of master image line segments, the gray values of the windows on slave image line segments need to be resampled. Then, we can use Normalized Cross Correlation (NCC) to evaluate the similarity of line segments in neighboring regions.

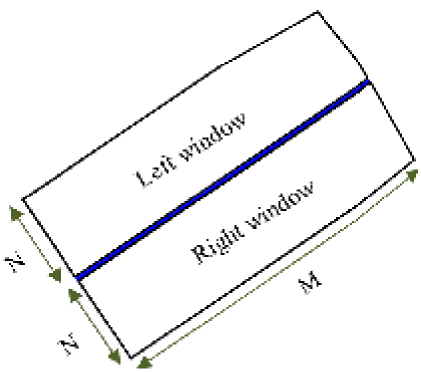

Figure 5: The illustration of the Left and Right window.

Multi-Plane Intersection

In this stage, we use those successfully matched lines with multi-plane intersection to generate 3D line segments. Since more than one matched lines on slave image may happen for each line segments, the consistency of lines should be check. The first step is to select one line segments at time on each slave image, and then intersect to objects space by multi-plane intersection for the selection lines. If there is existed a wrong matched line, the error of intersection would be larger than the others. The illustration of multi-plane intersection is shown in Figure 6.

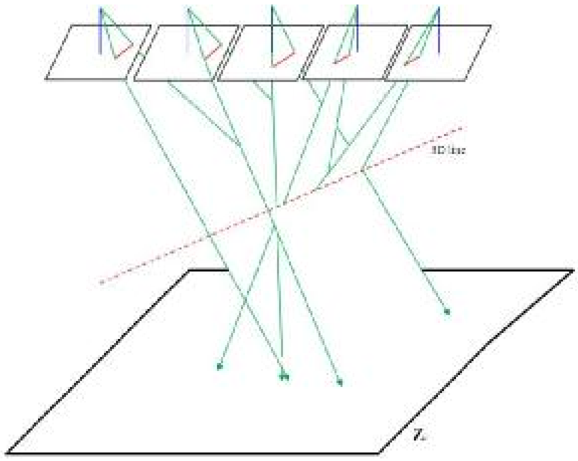

Figure 6: The illustration of Multi-Plane Intersection.

3. EXPERIMENTAL RESULTS

The data were obtained from DMC II images with the 10cm resolution. The target building on multiple images of case 1 with single strip are shown in Figure 7. The target building on multiple images of case 2 with double strips are shown in Figure 8.

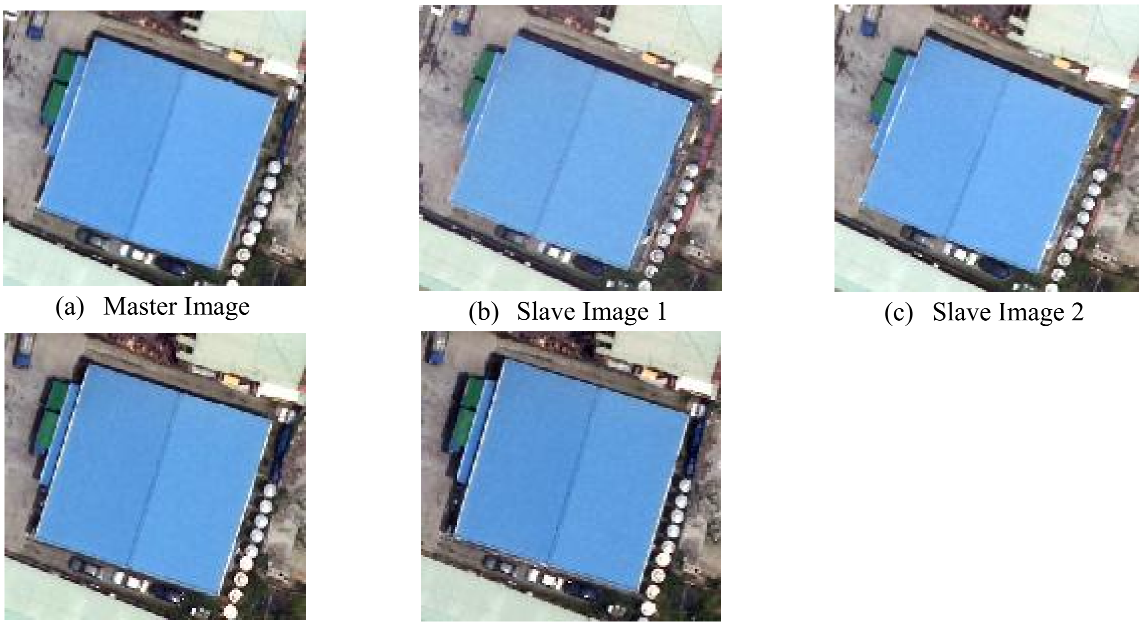

(a) Master Image
(b) Slave Image 1
(c) Slave Image 2
(d) Slave Image 3
(e) Slave Image 4

Figure 7: The target building on multiple images with single strip in Case 1.

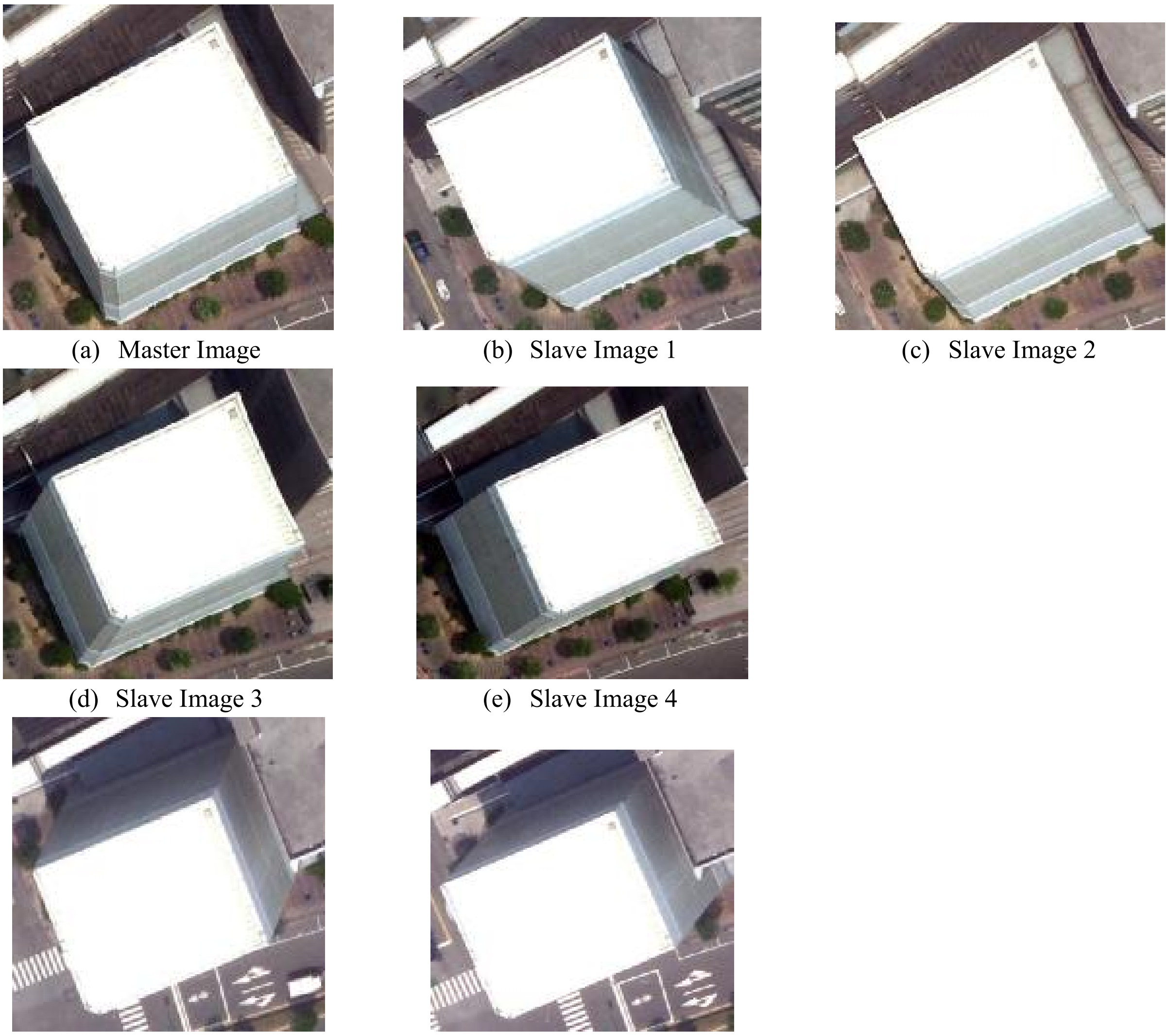

(a) Master Image (b) Slave Image 1 (c) Slave Image 2

(d) Slave Image 3 (e) Slave Image 4

(f) Slave Image 5 (g) Slave Image 6

Figure 8: The target building on multiple images with double strips in Case 2, (a) to (e) are the first strip images, (f) and (g) are the second strip images.

In the first part, the images are employed to Canny edge detection and Hough transform to generate line segments. Following the criteria of angle and distance, 27 and 14 lines are selected on master image in Case 1 and Case 2, respectively. The selected lines are shown in Figure 9.

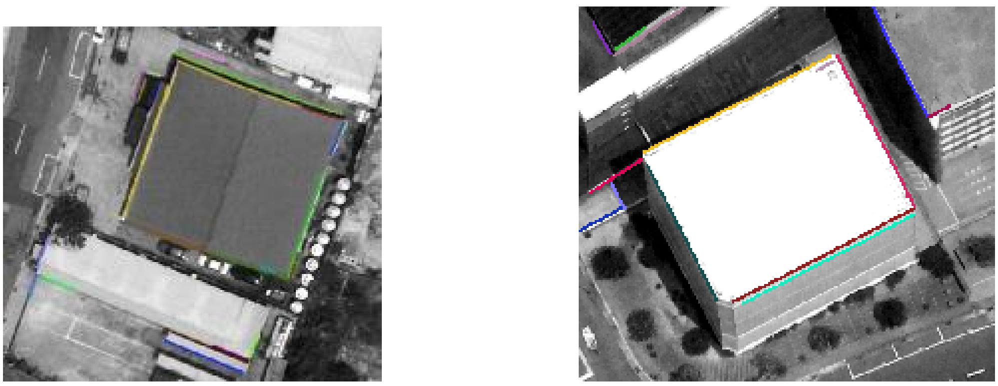

(a) (b)

Figure 9: The results of selection lines on master image, (a) Case 1, (b) Case 2.

In the window size determination, the matching results would be affected by the different N value. The statistics of the matching results in Case 1 and Case 2 are shown in Table 1 and Table 2, respectively. The front number represents the number of wrong match lines, and the after number means the all lines that are matched on slave image. After line matching, the 3D line segments can be constructed. The 3D line segments of Case 1 and Case 2 are shown in Figure 10 and Figure 11, respectively. The RMSEs of the corners can be obtained from comparing the generated 3D coordinates and the stereo measurement of 3D building models. The RMSEs of the building corners are shown in Table 3.

Table 1: The statistics of the matching results in Case 1.

Slave Image	n = 3	n = 5	n = 7	n = 9	n = 11	n = 15
1	0/10	0/8	0/8	0/9	0/8	0/8
2	0/13	0/14	0/13	0/11	0/11	0/12
3	0/11	0/11	0/11	0/11	0/12	0/13
4	1/13	1/12	2/13	2/13	2/13	0/12

* The front number represents the number of wrong match lines, and the after number means the all lines that are matched on slave image.

Table 2: The statistics of the matching results in Case 2.

Slave Image	n = 3	n = 5	n = 7	n = 9	n = 11	n = 15
1	0/8	0/6	0/6	0/6	0/6	0/7
2	0/8	0/8	0/8	0/8	0/8	0/6
3	0/9	0/9	0/8	0/9	0/8	0/8
4	1/9	0/8	0/7	0/7	0/6	0/7
5	1/7	1/5	1/5	1/6	1/6	1/5
6	0/7	1/3	1/3	1/3	1/4	0/2

* The front number represents the number of wrong match lines, and the after number means the all lines that are matched on slave image.

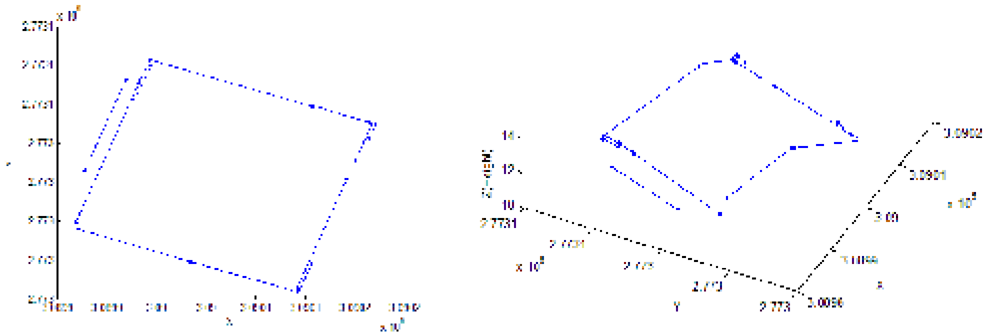

(a) (b)

Figure 10: The 3D line segments of Case 1, (a) vertical view, (b) side view.

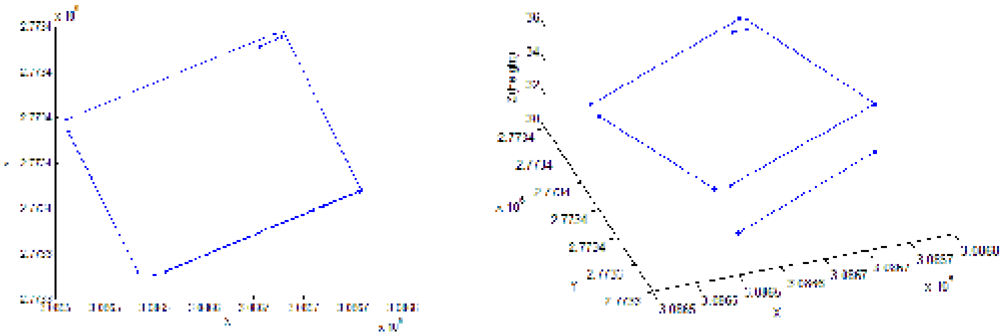

(a) (b)

Figure 11: The 3D line segments of Case 2, (a) vertical view, (b) side view.

Table 3: RMSEs and difference of building corners in object space.

	$RMSE_X$ (m)	$RMSE_Y$ (m)	$RMSE_Z$ (m)	Mean of Difference (m)
Case 1	0.228	0.266	0.385	0.239
Case 2	0.185	0.232	0.383	0.265

4. CONCLUSIONS & RECOMMENDATIONS

This study has proposed a scheme for line matching using Left-Right matching, and the construction of 3D lines segments can be derived from multi-plane intersection. The experimental results indicate that the proposed method is applicable. Compared with the manual measured models, the mean difference is under 0.3m. On the other hand, the accuracy of the 3D line segments could achieve accuracy under 0.3m in the horizontal and under 0.4m in vertical direction. In this study, the major target is constructing the building edge. However, there may be other inner structures on the roof, the detection of line features on the roof are to be considered after the reconstruction of 3D building boundaries. Since there are still matching ambiguities, the proposed method needs to be improved in the future.

REFERENCES:

Canny, J., 1986, A Computational Approach to Edge Detection, IEEE Transactions on Pattern Analysis and Machine Intelligence, 8(6), pp. 679-698.

Hough, P.V.C., 1962, Methods and Means for Recognizing Complex Patterns. U.S. patent No. 3069654.

Hsu, W. C., 1999. Building Extraction from Color Aerial Stereo Photo Pairs, Master degree dissertation, National Central University, Taiwan. (In Chinese)

Ok, A. O., Wegner, J. D., Heipke, C., Rottensteiner, F., Soergel, U., and Toprak, V., 2010. A new straight line reconstruction methodology from multi-spectral stereo aerial images. Saint-Mandé, France, September 1-3, 2010, IAPRS, Vol. XXXVIII, Part 3A.

Ok, A. O., Wegner, J. D., Heipke, C., Rottensteiner, F., Soergel, U., and Toprak, V., 2010. A stereo line matching technique for aerial images based on a pair-wise relation approach. International Archives of Photogrammetry and Remote Sensing, 38(1/W17), Istanbul (on CD-ROM).

Schmid, C. and Zisserman, A., 1997. Automatic Line Matching Across Views. In: Proceedings of CVPR, pp. 666-671.

Suveg, I., and Vosselman, G., 2004. Reconstruction of 3D Building Models from Aerial Images and Maps, ISPRS Journal of Photogrammetry and Remote Sensing, 58, pp. 202-224.